Powder Technology, Volume 336, August 2018, pp. 122-130
DOI:10.1016/j.powtec.2018.05.029

Accepted Manuscript

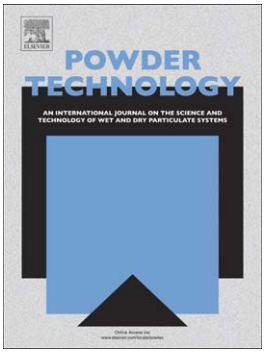

Estimation of powder mass flow rate in a screw feeder using acoustic emissions

C. Ruiz-Carcel, A. Starr, E. Nsugbe

PII: S0032-5910(17)30554-5
DOI: doi:10.1016/j.powtec.2017.07.015
Reference: PTEC 12657

To appear in: *Powder Technology*

Received date: 6 April 2017
Accepted date: 5 July 2017

Please cite this article as: C. Ruiz-Carcel, A. Starr, E. Nsugbe, Estimation of powder mass flow rate in a screw feeder using acoustic emissions, *Powder Technology* (2017), doi:10.1016/j.powtec.2017.07.015

Estimation of powder mass flow rate in a screw feeder using acoustic emissions

C. Ruiz-Carcel[a]; A. Starr[a]; E. Nsugbe[a]

[a] Through-Life Engineering Services Institute; Cranfield University, UK
Corresponding author: +44(0)1234755566 email: c.ruizcarcel@cranfield.ac.uk

Abstract

Screw feeders are widely used in powder processes to provide an accurate and consistent flow rate of particles. However this flow rate is rarely measured or controlled. This investigation explores the use of generalised norms and moments from structural-borne acoustic emission (AE) measurements as key statistics indicators for the estimation of powder mass flow rate in a screw feeder.

Experimental work was carried out acquiring AE measurements from an industrial screw feeder working with four different types of material at different dispensation rates. Signal enveloping was used in first place to eliminate high frequency components while retaining essential information such as peaks or bursts caused by particle impacts. Secondly a set of generalised norms and moments is extracted from the signal, and their correlation with mass flow rate was studied and assessed. Finally a general model able to estimate mass flow rate for the four different types of powders tested was developed.

Keywords: *powder flow; acoustic emission; screw feeder; process monitoring; signal analysis*

1. Introduction

Screw feeders are widely used in industries such as mining, metallurgy, food processing, pharmaceutical and consumer goods to draw bulk materials from storage containers and transfer them over a short distance [1]. In most cases it is critical to feed powders consistently and accurately into subsequent unit operations of the process line, as feeding is typically the first unit operation [2]. Real time process and product quality control is nowadays essential in any modern production line. The early detection of quality deviations enables a more efficient and dynamic process management, enhancing efficiency and final product quality. Measuring the amount of material (raw materials, additives, finished product) travelling through a specific process section can provide vital information. If this information is accurate and provided on-line in real time, it can be fed back into the process to control process parameters affecting the final quality of the product. However this is not an easy task when dealing with bulk materials such as fine powders composed of particles of different shapes, sizes, densities and chemical composition.

The measurement of particle mass flow rate has been addressed using different types of sensing technologies [3] based on measurements of electrostatic charge [4,5], microwaves [6], radiological emissions [7] or tomography [8,9]. In addition acoustic emission (AE) has been used in many previous research studies [10–14] with great results. The main benefits of AE compared to other sensing technologies include its non-intrusive nature [13], high sensitivity to particle impact in the vicinities of the sensor, and robustness against noise and other disturbances from the system when using high-frequency ultrasonic sensors [15]. On the other hand the high sampling rates required and the expertise for handling and processing heavy datasets are the main drawbacks of this technique.

In [11] a model was presented that explains how particle-wall collisions and friction generate AE, and the model was validated with experimental results. A signal decomposition based method allowed the authors to estimate mass flow rate. Albion et al. [13] presented a method

for determining flow regime in horizontal pneumatic transport using microphones. This method proved to be successful, but the use of acoustic measurements in the audible range makes it potentially prone to signal contamination from other sound sources [15] in an industrial environment, and the use of wavelet decomposition makes it computationally heavy. This problem was also studied in [12] where mass flow rate in abrasive jets using acoustic emission was estimated using two different methods. The first method was based on peak count with a dynamic threshold while the second approach estimated mass flow rate as a function of the power spectrum density of the signal. Both methods proved to be successful, but the peak count based method is only applicable when the frequency of the particles hitting the surface is much smaller than the plate ringing frequency. The relationship between signal power and the average number of particles impinging on a surface per unit of time was modelled in [10], and the accuracy of the model was corroborated with experimental data. A similar approach was presented in [15], where mass flow rate in an air conveyed horizontal pipe was correlated with the RMS value of AE signals.

Measuring particle flow rate in an industrial screw feeder presents additional challenges, as the AE activity is not mainly produced by individual particles hitting a surface but by the friction generated by a large group of particles with different characteristics being dragged by the screw over a surface at the same time. Additionally the estimation of mass flow rate in powders with a wide particle size distribution can be difficult due to the large differences in the acoustic activity generated by these particles. The development of a flow rate estimation method valid for powders with different compositions and physical properties is complicated for the same reasons. These were the main challenges faced in this investigation.

The data processing method proposed in this paper aims to deepen in the concept presented in [10,15] of stablishing a relationship between particle flow rate and general signal

characteristics (such as RMS) that can be obtained with very limited computational cost. In first place the envelope of the signal is calculated to eliminate fast oscillations while retaining a smooth curve outlining its extremes, which contains essential information such as the presence of peaks or bursts caused by particle impacts. This smooth curve without very high frequency components does not require a sampling rate as high as the original signal to be accurately represented. This step allows an enormous reduction in the size of the data set to be analysed subsequently and makes it more suitable for real time estimations. Secondly, basic time-domain features such as generalised norms and moments are extracted from the signal, which can be correlated with physical parameters such as flow rate. This method was tested and assessed using experimental data acquired from a screw feeder working at different speeds and with powders of different physical characteristics, generating a general data-based model able to estimate mass flow rate for different powders according to their bulk density.

The rest of the paper is structured as follows: section 2 explains in detail the signal processing methodology proposed. The experimental set up is described in section 3, including information about the experimental rig and the experiments carried out. The results obtained are presented and discussed in section 4. Finally the work is concluded in section 5.

2. Methodology

Acoustic emission is defined as transient elastic waves generated by the sudden release of energy from localised sources within a material [16]. Plastic deformation, crack propagation, erosion, corrosion, impacts and leakage are the most common sources of AE. These waves are characterised generally by a very high frequency and low amplitude signal. Piezo-ceramic sensors are widely used because of their high sensitivity and robustness. The mechanical resonance of the detecting element in the sensor is used to obtain high sensitivity to these

weak waves, although in some cases a damping element is bonded around the detecting element to generate a flatter frequency response [17].

The signals produced by particle interactions generate a series of high-frequency bursts in the captured signals as resonance frequencies are excited by particle impacts. Although the signal is dominated by the resonance frequencies excited, the relevant information is contained in the characteristics of these bursts such as their amplitude, duration, the number of event repetitions, etc. For that reason, in this investigation the AE signals acquired were first demodulated to obtain the envelope and remove the resonant components of the signal. Secondly the characteristics of the envelope were analysed to study the correlation between powder flow rate and AE.

2.1 Signal Enveloping

High frequency bursts in an AE signal can be modelled as an amplitude modulation of a carrier signal at the resonance frequency by a series of exponential pulses. The signal envelope can be extracted by amplitude demodulation to reveal the overall characteristics of these bursts. The envelope can be extracted using the Hilbert transform as a resonance demodulator. It can also be estimated by integrating the absolute value of the signal over a period of time or calculating the moving maximum of the signal over a sliding window. In these cases, the time constant can be chosen by the analyst according to the requirements allowing a more flexible analysis. Long time-constants can reveal long-term trends of the overall level of AE activity, while for short time-constants the output will be a dynamic representation of the variations in the AE signal magnitude. Fig. 1 shows an example of these methods where the original signal is compared to its envelopes obtained using the Hilbert transform and a moving maximum sliding window of 25 data points.

From Fig. 1 it can be seen how both enveloping methods are capable of reproducing the overall amplitude variations in the original signal while ignoring the high frequency oscillations. In this investigation the "moving max" method with a window length of 25 data points was used due to its ability to represent more accurately the amplitude of sharp signal bursts, such as the burst starting after 2 ms in Fig. 1.

2.2 Extraction of basic statistical signal features: generalised norms and moments

Statistical analysis provides various features for the signals: norms and moments are commonly used in developing time-domain based features [18]. Absolute mean and root mean square (RMS) are examples of commonly used norms. Normalised (dimensionless) moments around the mean skewness and kurtosis are special cases corresponding to orders three and four respectively, and are commonly used in vibration analysis [18].

Higher order norms and moments can be more sensitive to impact-like phenomena as the high exponent magnifies large signal values against "carpet level" values. Higher order derivatives provide additional methods for vibration analysis [18]. As an example, the first time derivative of acceleration, known as jerk, has been used for assessing the comfort of travelling, for example in designing lifts, and for slowly rotating rolling bearings [19]. These characteristics are very interesting for this particular case study, which aims to characterise the bursts produced in AE signals due to particle impact and find a correlation with powder mass flow rate.

For a discrete random variable X, having possible values x_i , $i = 1,\ldots,N$, the probability of each value is defined by a probability function $P(X = x_i)$. A signal $x(t)$ is a sample with a length of T from a continuous variable X. Values are selected from the signal with an equal-

sized time interval T/(N–1). The probability of each value is defined by a density function $f(x)$, ie $P(X = x_i) = f(x_i)$, and the expectation of X is defined by:

$$E(X) = \sum_{i=1}^{N} x_i P(X = x_i) = \sum_{i=1}^{N} x_i f(x_i) \tag{1}$$

A norm $\|M\|$ of signal x with sample time τ is defined by:

$$\left\| {}^{\tau}M_{\alpha}^{p} \right\| = ({}^{\tau}M_{\alpha}^{p})^{1/p} = \left(\frac{1}{N} \sum_{i=1}^{N} \left| x_i^{(\alpha)} \right|^{p} \right)^{1/p} \tag{2}$$

where $p \neq 0$ and represents the norm order and α represents the derivation order. It has same dimensions as the corresponding signals $x^{(\alpha)}$.

The mean is the first moment about the origin. Higher moments M^p about the origin can be defined as expectations $E(X^p)$. The moments can also be defined about some central value $c \in \mathbb{R}$, for example the moments about the mean $\bar{x}$ are defined by:

$${}_{\sigma}^{\tau}M_{\alpha}^{k} = \frac{1}{N(\sigma_{\alpha})^{p}} \sum_{i=1}^{N} \left| x_i^{\alpha} - \bar{x}^{(\alpha)} \right|^{p} = \frac{1}{N} \sum_{i=1}^{N} \left| \frac{x_i^{\alpha} - \bar{x}^{(\alpha)}}{\sigma_{\alpha}} \right|^{p} \tag{3}$$

The generalised central absolute moment about $c = \bar{x}^{\alpha}$ can be normalised by means of the standard deviation σ_{α} of the signal $x^{(\alpha)}$ to make it dimensionless.

This procedure described in detail in [18] was used in this investigation to compute a range of norms and moments of the acquired AE signals and their derivatives. The correlation between these individual features and the measured mass flow rate was studied in order to obtain the model that best estimates flow rate from the AE signal characteristics.

3. Experimental set up

3.1 Testing hardware and instrumentation

An Ajax screw feeder size 75 (diameter 75mm) was used for the experiment (Fig. 2). It consist of a hopper where the powder is stored and a screw driven by a motor and a gearbox which displaces the material towards the discharge. This machine is used in different industrial applications to provide a consistent flow rate of powder. However it is not equipped with any kind of sensor to measure this flow rate in real time. The machine is equipped with a variable speed drive to adjust the flow rate provided. The nominal speed of the motor is 1360 rpm at 50 Hz, and it is attached to a gearbox with a reduction ratio of 47:1. A Physical Acoustics D9241A differential sensor was attached to the outside of the screw's cover (Fig. 3). Dow Corning 3140 RTV coating was used as a couplant to maximise signal transfer to the sensor without modifying or damaging the surface. This sensor has an operating bandwidth of 10-100KHz. The AE signal from the sensor was preamplified 40 dB before being digitised using a PicoScope 4224-11 oscilloscope at a sampling rate of 1 MHz.

3.2 Summary of tests carried out

The proposed approach was tested with AE signals acquired from the feeder. Four types of powders with different compositions and densities (see Table 1) were used during the tests. These powders are raw materials (sodium sulphate) or intermediate products (blown powder produced in a drying tower) in the washing powder production. The objective is to assess the capabilities of the algorithm for different types of powder. Fig. 4 shows the particle size distribution of the four powders tested. These particle size distributions were obtained by sieving the powder with 10 sieves of different sizes.

The experiments were carried out at four different speed set-points, selected by changing the frequency of the current fed to the motor. AE signals sampled at 1MHz were acquired for every possible combination of powder and speed. Each of these tests was repeated 10 times to produce a significant amount of data and cope with measurement uncertainties (see Table 2).

Fig. 5 shows an example of the signals acquired for powders 1 and 3 (highest and lowest densities tested) with flow rates 1 and 4 (lowest and highest speeds tested). These examples show how the signal peak amplitude is higher for powders with higher density and higher speeds. It can also be seen how for powder 1 the fluctuations produced by the screw blade passing over the sensor location at 20 Hz and 50 Hz, but these fluctuations are not visible for powder 3.

4. Results

4.1 Flow rate measurement

The mass of powder coming out of the feeder was measured over periods of around 90 seconds to determine the mass per unit of time delivered by the feeder. These measurements were undertaken several times for each combination of powder and speed tested. Although short time flow rate fluctuations due to the effect of the screw's blades were observed for Powder 1, the overall flow rate measured over a longer time span was constant and repeatable. Additionally, there is a linear correlation between the speed and the mass flow rate for each one of the powders tested. This was an expected result as the volume displaced per screw revolution can be considered constant. The results obtained are summarised in Table 3, and will be used to calibrate the method proposed, trying to find a correlation between AE signal features and actual flow rate.

4.2 Selection of data set length

The original 20 s observations were split in smaller sections in order to observe how the length of the data set acquired affects the accuracy of the method, and select the minimum sample size possible without compromising it. This step also generates a richer data set, increasing the number of observations and the reliability of the model fitted. The procedure described in section 2.2 was used to obtain generalised norms and moments of enveloped

signals of different sizes for this analysis. The features obtained were correlated with the measured flow rates, and a linear model was fitted through the data points, in an attempt to correlate AE features and mass flow rate. The accuracy of the model was evaluated using the mean prediction error, calculated as the average absolute differences between observed values and model estimations, expressed as percentages of the observed value. Fig. 6 shows the evolution of the prediction error of the first norm (p=1) of the original signal (α=0).

The results presented in Fig. 6 show that the prediction error decreases as the sample size increases, until a certain point where the model reaches maximum accuracy and the addition of observations has no effect in the prediction error. The minimum error achievable is lower for powders 1 and 4 (between 2 % and 3 %) and slightly higher for powders 2 and 3 (around 5%). The prediction error levels out for powder 2, 3 and 4 with observations of around 10.000 samples. Powder 1 however requires a higher number of samples per observation to achieve maximum accuracy, around $2x10^6$ samples. This is attributed to the big fluctuations observed in the AE signal for powder 1 due to the screw blade effect (see Fig. 5), requiring a number of samples that covers at least one of this oscillations to produce repeatable results. Similar results were obtained for other norms and derivative orders. In practical terms, a sample length of 2 s was selected as a result of this analysis.

The original 20 s signals acquired were split in sections of 2 s ($2x10^6$ samples at 1MHz) for all the powders and speeds tested, generating 400 observations for each type of powder. Even numbered observations were used for algorithm training, fitting a linear curve through these points. Odd observations were used to assess the accuracy of the model by looking at the prediction error of these observations for each case studied.

4.3 Estimation of powder flow rate through generalised norms.

The procedure described in section 2.2 was used to obtain generalised norms for all the enveloped AE observations, up to norm order 6 (p=6) and derivation order 5 (α=5). Fig. 7

shows an example of the results obtained for generalised norms up to order 3 and derivation order 2 for powder 1. This figure shows the samples used for training (blue) as well as the monitoring samples (red), and the estimations provided by a linear model in each case (green).

These results show how the features obtained from different norms and derivative orders have a relative high correlation with mass flow rate, producing estimation errors in the order of 2%. Performing the analysis on high order derivatives seems to have a negative effect on the correlation, as the prediction error increases slightly with the derivation order in most cases. However higher norm orders tend to reduce the estimation error, improving the accuracy of the method. These results can also be observed in the other powders tested. Tables 4 to 7 summarise the estimation error obtained for all the norms studied in the 4 powders tested.

4.4 Estimation of powder flow rate through generalised moments

The same analysis used in the previous section was performed using generalised moments up to moment order 8 (the first moment considered was order 3) and up to derivation order 5 (α=5). Fig. 8 shows an example of the results obtained for generalised moments up to order 5 and derivation order 2 for powder 1. This figure shows the samples used for training (blue) as well as the monitoring samples (red), and the estimations provided by a linear model in each case (green).

These results show how the features obtained from different moments and derivative orders have a poor correlation with powder flow rate in most cases, and in those cases where correlation exists it is not as good as it was for generalised norms. Quadratic and exponential models were also used in addition the linear model shown here, but the error rates obtained were not massively improved due to the large scatter on the data points. Tables 8 to 11 summarise the estimation error obtained for all the moments studied in the 4 powders tested.

Performing the analysis on high order derivatives had different effects for the different powders tested. In most cases increasing the derivation order did not improve the model accuracy, but for powders 2 and 3 the 2^{nd} and 4^{th} derivation orders seem to produce slightly better results among the moments studied. Increasing the moments' order did not have a general benefit over the model accuracy in general. The lowest estimation errors are normally found for the 3^{rd} or 4^{th} moments. High order moments tend to magnify in excess samples containing relatively high values, reducing the accuracy of the linear curve fitting on the training samples.

4.5 Density-dependant model for all powders

During the analysis of the results obtained from generalised norms it was noted that the coefficients of the linear curves fitted changed accordingly with the density of the powders tested. In an attempt to produce a general model for any kind of powder as a function of its density, the coefficients of the linear curves fitted on the training data were plotted against the density of the powders studied. For simplicity and repeatability, the coefficients obtained from the first norm of the original enveloped signals (derivative order 0) were used. Fig. 9 shows the evolution of the linear and independent terms against the powder density for each of the 4 powders studied.

These results were used to produce a general model able to estimate mass flow rate for different types of powders using the powder density as an input. Fig. 10 shows the results obtained for mass flow rate estimation using this density-based model.

In terms of model accuracy, the results obtained with the density-based model are quite similar for powders 1 and 2 to the best possible fit across the data points. For powders 3 and 4 the average estimation error is slightly higher (around 1 %) with the density based model, but still produces quite accurate results. The use of this model allows the estimation of powder

flow rate in a screw feeder when powders of different densities are used once the model is trained, using only bulk density as an input for the model.

5. Conclusion

In this investigation work a set of generalised norms and moments was extracted from enveloped AE signals to determine if there is a correlation between these features and powder flow rate in a screw feeder. The results show that norms extracted from enveloped signals of 2s of length or more are highly correlated with the mass flow rate for different types of powders. This correlation allows the estimation of powder flow rate from AE signals. Increasing the norms' order improves the accuracy of the model by between 0.3 % and 1.4 %, but applying the method on high order derivatives had poorer accuracy. On the other hand the correlation between generalised moments and mass flow rated proved to be much weaker than for generalised norms. Although in some cases the accuracy of the model was acceptable, such as moments 3 and 4 for the original signals from powder 4, most of the features studied shown poor correlation with estimation errors up to 35%. In addition there is no clear benefit on using high order moments, the minimum errors were found for moments 3 and 4 in most of the cases studied.

Finally, the correlation between the coefficients of the linear models found for generalised norms and powder density was studied, and a general model for different types of powders was implemented using density as an input. The results showed that this density-based model is slightly less accurate than individual models for each powder with an average 0.54% increase in the prediction error, but the estimations are still acceptable. The use of this model

is hugely beneficial, as it allows the estimation of mass flow rate of different powders based on AE measurements using powder density as an input.

The methodology presented in this investigation work demonstrates how powder mass flow rate can be measured in a screw feeder using AE, a non-intrusive technology, applying a basic and computationally efficient algorithm. The results showed that high order norms can produce more accurate estimations than RMS using AE measurements of 2 s. The accurate flow rate estimation results obtained from generalised norms of AE signals fulfil the objectives of this research work.

Additionally, the development of a general model based on AE features and powder density provided a flexible flow rate estimation tool for different types of materials. In a real application the signal enveloping used here prior to the data analysis can be done before data collection using an analogue enveloper, allowing for a much lower sampling rate. With this approach it will be possible to measure powder flow rate on-line and in real time, which potentially allows the use of these flow rate estimations for real time process monitoring and control.

Acknowledgements

The authors gratefully acknowledge the support of AMSCI for funding this research via the Chariot Consortium. The Advance Manufacturing Supply Chain Initiative is a government supply chain fund which is helping to rebuild British manufacturing prowess. The contribution of CPI for hosting the experiments, Ajax for manufacturing the screw feeders and P&G leading the Chariot project is gratefully acknowledged.

References

1. Hou QF., Dong KJ., Yu AB. DEM study of the flow of cohesive particles in a screw feeder. Powder Technology. 2014; 256: 529–539.
2. Wang Y., Li T., Muzzio FJ., Glasser BJ. Predicting feeder performance based on material flow properties. Powder Technology. 2017; 308: 135–148.

3. Yan Y. Mass flow measurement of bulk solids in pneumatic pipelines. Measurement Science and Technology. 1996; 7(12): 1687–1706.

4. Xu C., Wang S., Tang G., Yang D., Zhou B. Sensing characteristics of electrostatic inductive sensor for flow parameters measurement of pneumatically conveyed particles. Journal of Electrostatics. 2007; 65(9): 582–592.

5. Peng L., Zhang Y., Yan Y. Characterization of electrostatic sensors for flow measurement of particulate solids in square-shaped pneumatic conveying pipelines. Sensors and Actuators, A: Physical. 2008; 141(1): 59–67.

6. Howard A V. Development of Techniques for the Measurement of Concentration and Mass Flow Rate of Pneumatically Conveyed Coal Dust. 1980.

7. Barratt IR., Yan Y., Byrne B., Bradley MSA. Mass flow measurement of pneumatically conveyed solids using radiometric sensors. Flow Measurement and Instrumentation. 2000; 11(3): 223–235.

8. Sun M., Liu S., Lei J., Li Z. Mass flow measurement of pneumatically conveyed solids using electrical capacitance tomography. Measurement Science and Technology. 2008; 19(4): 45503.

9. Zheng Y., Li Y., Liu Q. Measurement of mass flow rate of particulate solids in gravity chute conveyor based on laser sensing array [article]. Optics Laser Technology. March 2007; 39: 298–305.

10. Pecorari C. Characterizing particle flow by acoustic emission. Journal of Nondestructive Evaluation. 2013; 32(1): 104–111.

11. He L., Zhou Y., Huang Z., Wang J., Lungu M., Yang Y. Acoustic Analysis of Particle − Wall Interaction and Detection of Particle Mass Flow Rate in Vertical Pneumatic Conveying. 2014;

12. Ivantsiv V., Spelt JK., Papini M. Mass flow rate measurement in abrasive jets using acoustic emission. Measurement Science and Technology. 2009; 20(9): 95402.

13. Albion K., Briens L., Briens C., Berruti F. Flow regime determination in horizontal hydrotransport using non-intrusive acoustic probes. Canadian Journal of Chemical Engineering. 2008; 86(6): 989–1000.

14. Hou R., Hunt A., Williams RA. Acoustic monitoring of pipeline flows: Particulate slurries. Powder Technology. 1999; 106(1–2): 30–36.

15. Hii NC., Tan CK., Wilcox SJ., Chong ZS. An investigation of the generation of Acoustic Emission from the flow of particulate solids in pipelines. Powder Technology. Elsevier B.V.; 2013; 243: 120–129.

16. ASTM. E1316 − 16a: Standard terminology for nondestructive examinations. West Conshohocken, PA: ASTM International; 2016.

17. Holroyd TJ. The acoustic emission and ultrasonic monitoring handbook. First. Coxmoor Publishing company; 2000.

18. Lahdelma S., Juuso E. Signal processing and feature extraction by using real order derivatives and generalised norms. Part 2: Applications. International Journal of Condition Monitoring. 2011; 1(2): 54–66.

19. Smith JD. Vibration monitoring of bearings at low speeds. Tribology International. 1982; 15(3): 139–144.

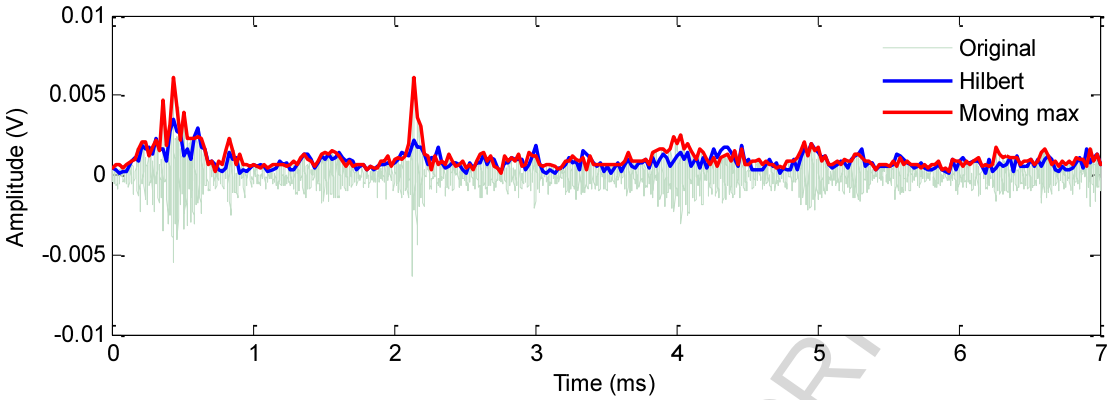

Fig. 1: Comparison of different enveloping methods

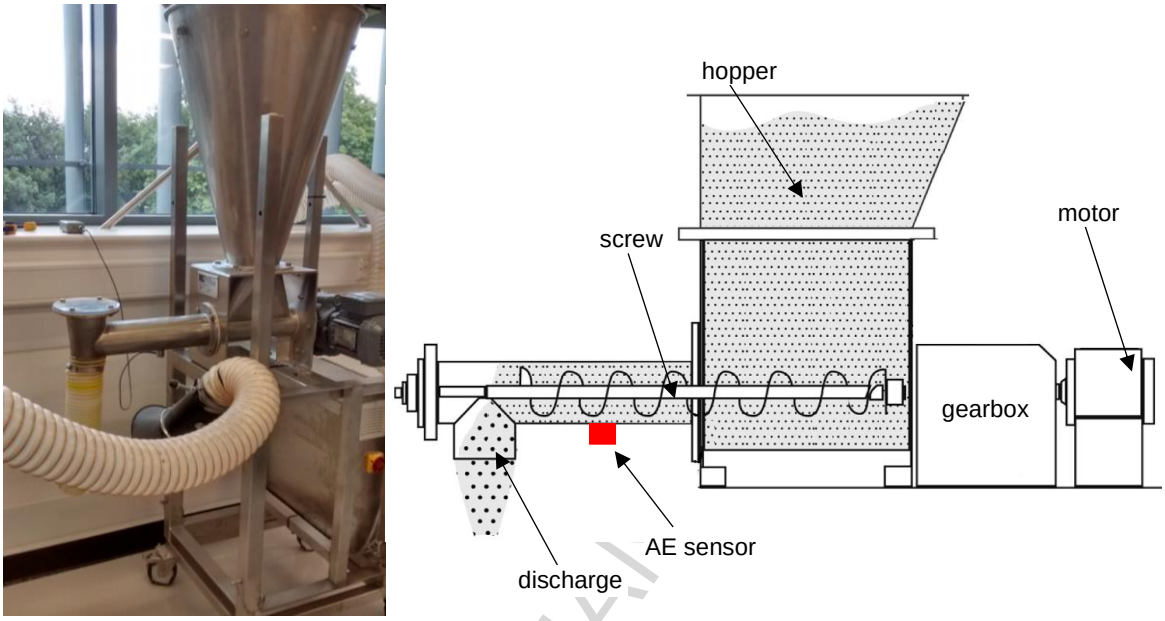

Fig. 2: Ajax screw feeder (left) and diagram (right)

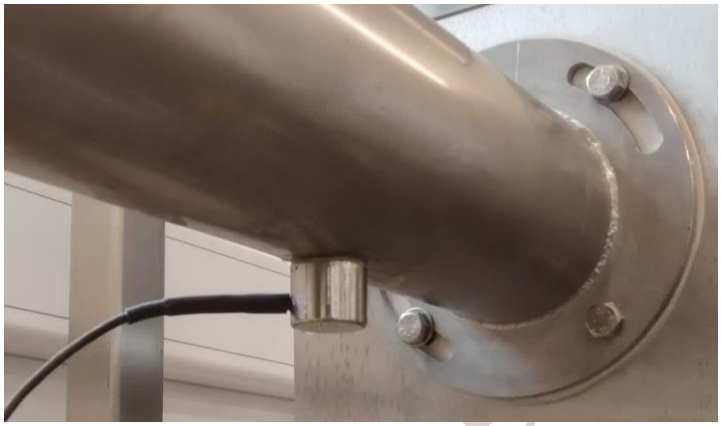

Fig. 3: Sensor installation detail

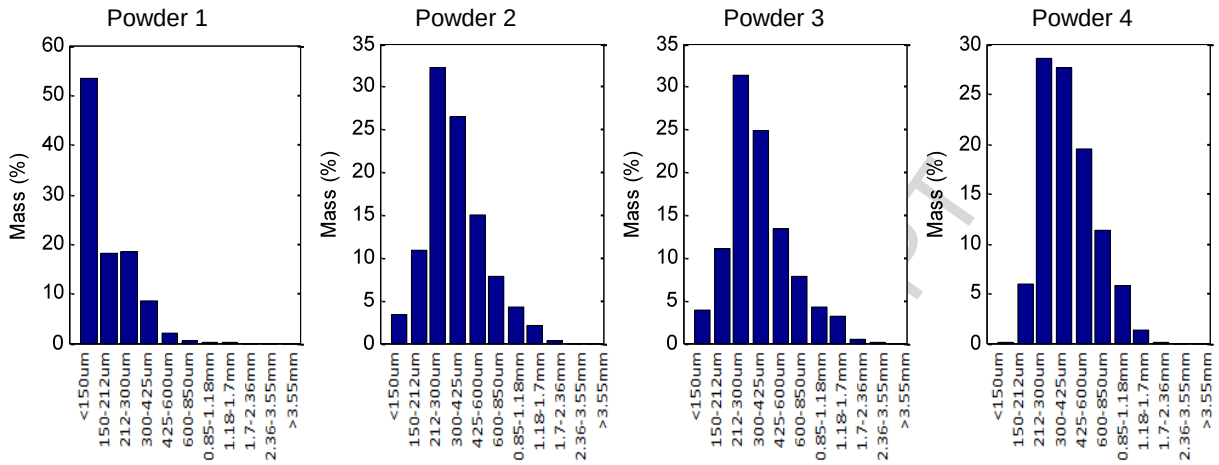

Fig. 4: Particle size distributions

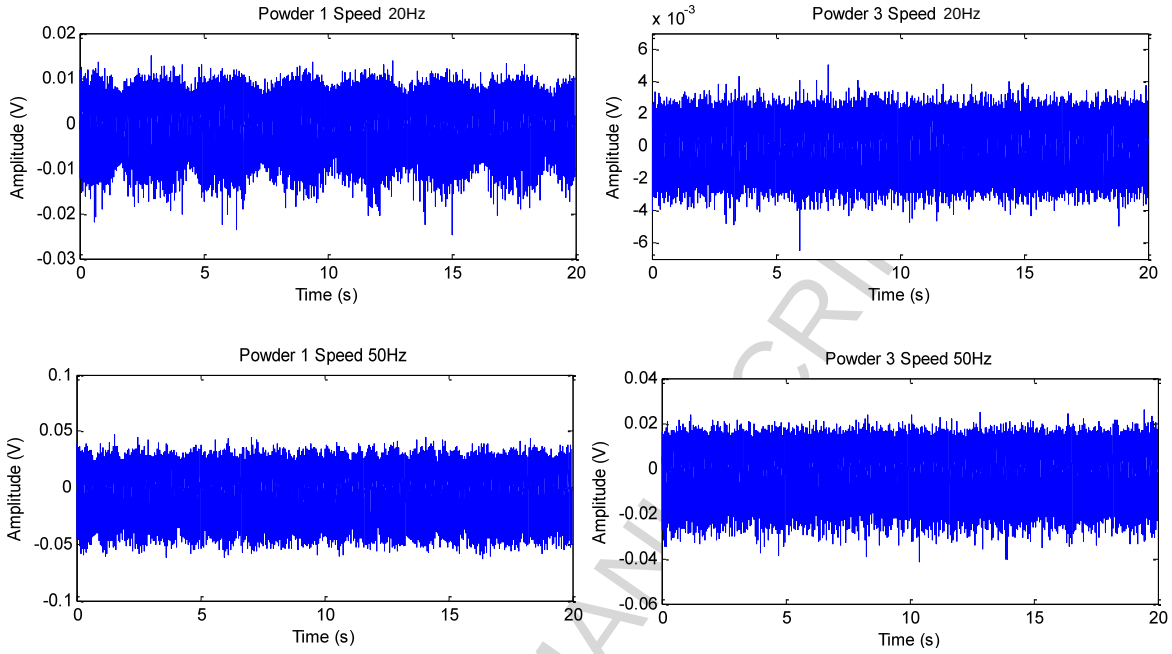

Fig. 5: Examples of signals acquired for powders 1 (left) and 3 (right) at 20Hz (top) and 50Hz (bottom)

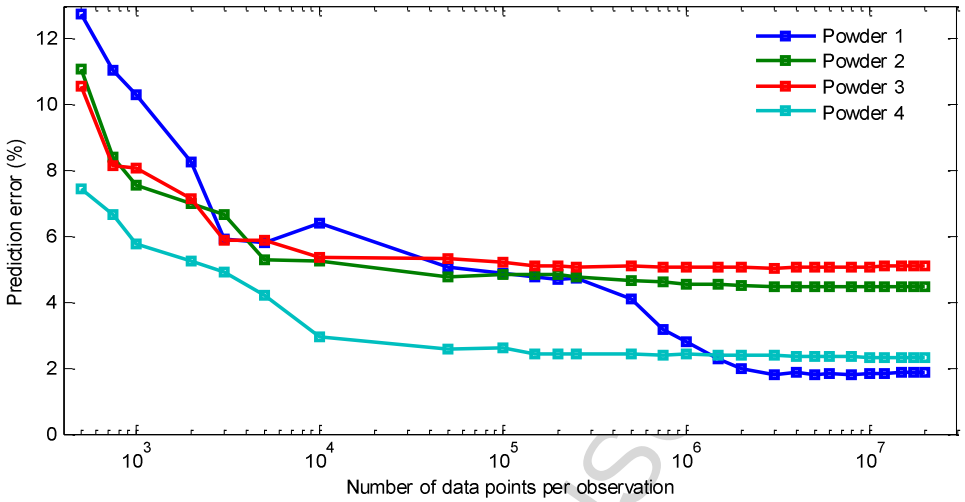

Fig. 6: Evolution of prediction error vs sample size for 1st norm, derivative order 0

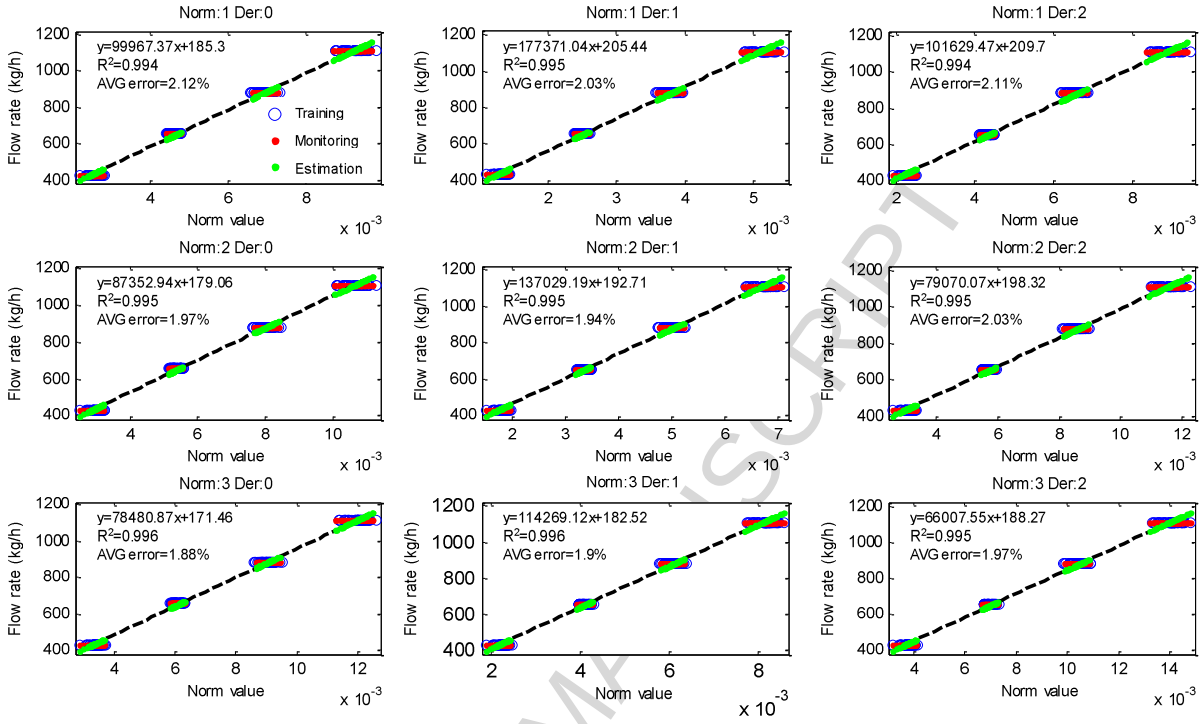

Fig. 7: Generalised norms vs flow rate for powder 1

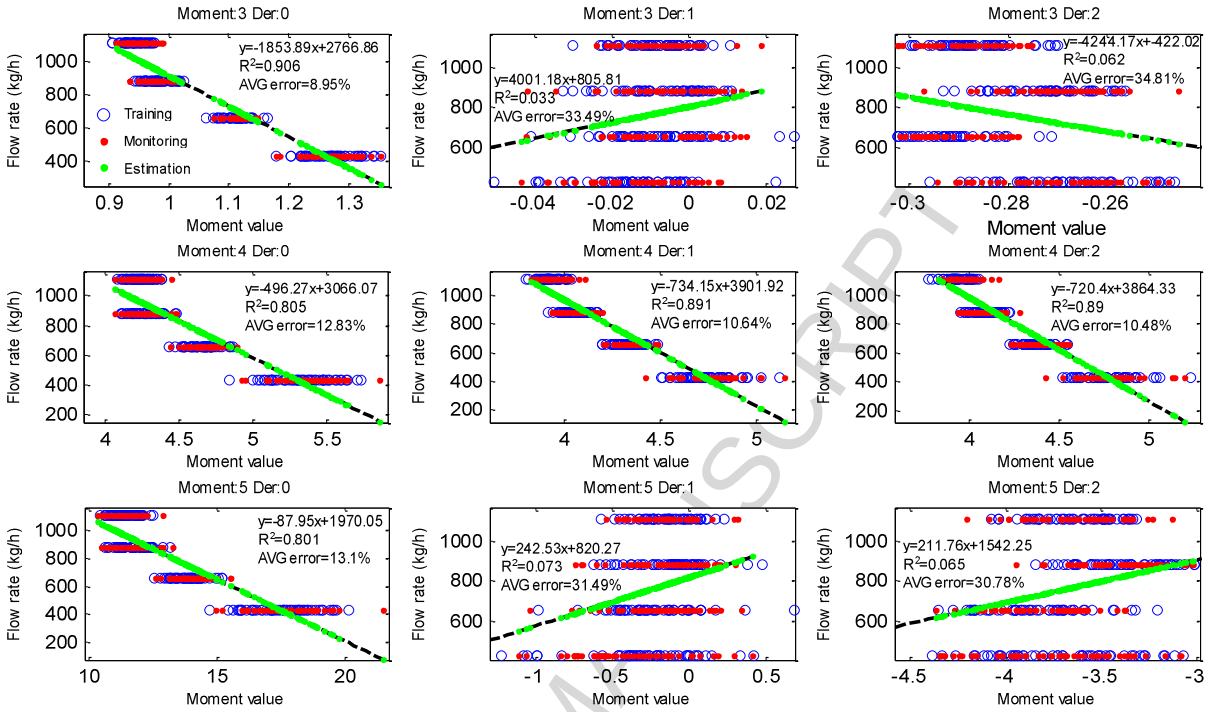

Fig. 8: Generalised moments vs flow rate for powder 1

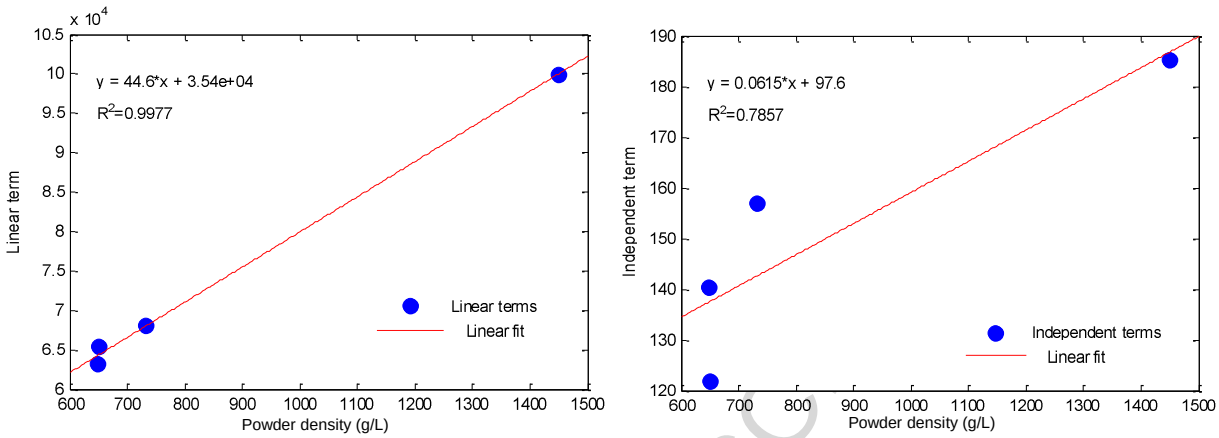

Fig. 9: Evolution of the linear term (left) and independent term (right) against powder density

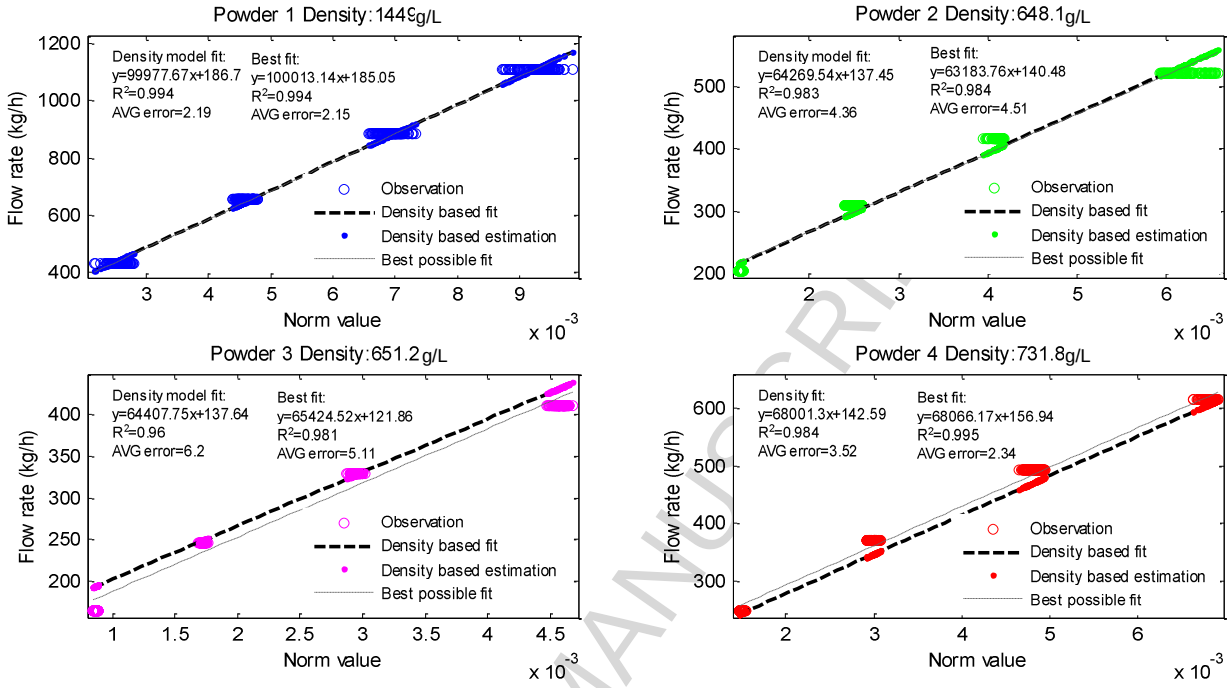

Fig. 10: Flow rate estimations using density-based model

Table 1: Density of powders tested

Powder ID number	Material	Bulk density (g/L)
1	Sodium sulphate	1449.0
2	Blown powder-high density	648.4
3	Blown powder-low density	561.2
4	Anionic agglomerate	731.8

Table 2: Experiment matrix

	Flow rate1 (20Hz)	Flow rate2 (30 Hz)	Flow rate3 (40 Hz)	Flow rate4 (50 Hz)
Powder 1	10x20s	10x20s	10x20s	10x20s
Powder 2	10x20s	10x20s	10x20s	10x20s
Powder 3	10x20s	10x20s	10x20s	10x20s
Powder 4	10x20s	10x20s	10x20s	10x20s

Table 3: Mass flow rates provided by the feeder (kg/h)

	Flow rate1 (20Hz)	Flow rate2 (30 Hz)	Flow rate3 (40 Hz)	Flow rate4 (50 Hz)
Powder 1	429.3	656.0	882.7	1109.4
Powder 2	202.4	309.3	416.3	523.2
Powder 3	163.9	246.2	328.6	410.9
Powder 4	249.0	370.7	492.4	614.1

Table 4: Estimation error for generalised norms in powder 1 (%)

	Der. 0	Der. 1	Der. 2	Der. 3	Der. 4	Der. 5
Norm 1	2.1	2.0	2.1	2.2	2.2	2.2
Norm 2	1.9	1.9	2.0	2.0	2.1	2.1
Norm 3	1.9	1.9	1.9	2.0	2.0	2.0
Norm 4	1.8	1.9	1.9	1.9	1.9	2.0
Norm 5	1.8	1.9	1.9	1.9	2.0	2.0
Norm 6	1.8	1.9	2.0	2.0	2.0	2.0

Table 5: Estimation error for generalised norms in powder 2 (%)

	Der. 0	Der. 1	Der. 2	Der. 3	Der. 4	Der. 5
Norm 1	4.5	4.6	4.8	4.9	5.0	5.0
Norm 2	4.2	4.2	4.5	4.6	4.7	4.7
Norm 3	3.9	3.9	4.2	4.3	4.3	4.4
Norm 4	3.6	3.7	3.9	4.1	4.1	4.2
Norm 5	3.5	3.6	3.8	3.9	3.9	3.9
Norm 6	3.3	3.5	3.6	3.7	3.8	3.8

Table 6: Estimation error for generalised norms in powder 3 (%)

	Der. 0	Der. 1	Der. 2	Der. 3	Der. 4	Der. 5
Norm 1	5.1	5.6	5.9	5.9	6.0	6.0
Norm 2	4.9	5.2	5.4	5.5	5.6	5.6
Norm 3	4.6	4.8	5.0	5.2	5.2	5.3
Norm 4	4.3	4.5	4.7	4.8	4.9	4.9
Norm 5	4.0	4.3	4.5	4.6	4.6	4.6
Norm 6	3.7	4.1	4.3	4.4	4.4	4.4

Table 7: Estimation error for generalised norms in powder 4 (%)

	Der. 0	Der. 1	Der. 2	Der. 3	Der. 4	Der. 5
Norm 1	2.3	2.0	2.1	2.2	2.2	2.2
Norm 2	2.0	1.7	1.8	1.9	1.9	1.9
Norm 3	1.8	1.5	1.6	1.7	1.7	1.7
Norm 4	1.6	1.4	1.4	1.5	1.5	1.5
Norm 5	1.4	1.2	1.3	1.4	1.4	1.4
Norm 6	1.3	1.2	1.2	1.3	1.3	1.3

Table 8: Estimation error for generalised moments in powder 1 (%)

	Der. 0	Der. 1	Der. 2	Der. 3	Der. 4	Der. 5
Moment 3	8.9	33.5	34.8	33.4	25.3	31.9
Moment 4	12.8	10.6	10.5	10.2	10.2	10.2
Moment 5	13.1	31.5	30.8	33.7	33.9	32.1
Moment 6	15.0	13.6	13.6	13.2	13.4	13.7
Moment 7	17.0	31.9	27.0	33.8	35.1	32.8
Moment 8	19.2	17.7	17.7	17.4	17.7	18.0

Table 9: Estimation error for generalised norms in powder 2 (%)

	Der. 0	Der. 1	Der. 2	Der. 3	Der. 4	Der. 5
Moment 3	28.7	35.1	14.4	35.1	13.2	34.4
Moment 4	8.5	15.5	19.9	19.9	20.4	20.8
Moment 5	13.1	34.3	20.2	34.9	18.2	34.8
Moment 6	22.9	15.1	21.2	19.6	20.5	20.8
Moment 7	32.2	35.3	35.1	35.3	34.5	35.3
Moment 8	34.7	29.4	32.2	30.7	30.3	29.9

Table 10: Estimation error for generalised norms in powder 3 (%)

	Der. 0	Der. 1	Der. 2	Der. 3	Der. 4	Der. 5
Moment 3	29.9	21.3	12.6	25.6	11.0	32.4
Moment 4	29.1	33.7	33.3	33.3	33.1	33.0
Moment 5	31.9	28.8	14.9	33.5	13.2	32.0
Moment 6	30.8	32.6	33.5	33.4	33.7	33.7
Moment 7	37.4	33.5	26.7	33.7	25.1	32.8
Moment 8	44.2	34.7	35.0	32.9	33.2	33.5

Table 11: Estimation error for generalised norms in powder 4 (%)

	Der. 0	Der. 1	Der. 2	Der. 3	Der. 4	Der. 5
Moment 3	9.1	26.8	18.3	32.2	15.9	33.0
Moment 4	7.3	6.0	7.3	7.7	8.3	8.9
Moment 5	9.0	27.1	32.9	33.1	30.0	33.3
Moment 6	11.7	8.7	10.3	10.9	11.8	12.5
Moment 7	14.9	30.1	26.1	33.0	31.4	32.8
Moment 8	18.0	15.0	16.8	16.7	17.7	18.5

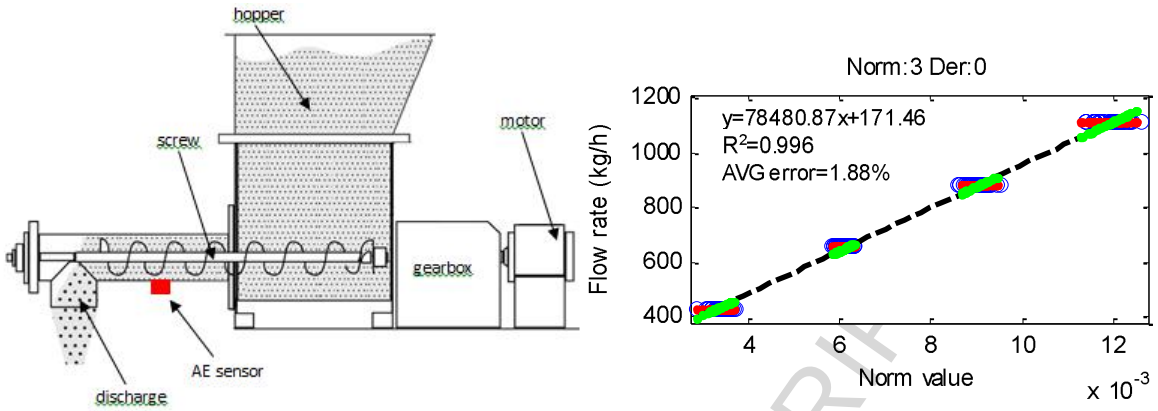

Graphical abstract

Highlights

- Generalised norms and moments from AE signals is proposed for flow rate estimation
- Signal enveloping is used to simplify data analysis
- The approach was tested on a screw feeder with different powders
- High order norms improve flow rate estimation accuracy
- A general density-based model is able to estimate flow rate of different powders

Estimation of powder mass flow rate in a screw feeder using acoustic emissions

Ruiz-Carcel, Cristobal

2017-07-08

Ruiz-Carcel C, Starr A, Nsugbe E, Estimation of powder mass flow rate in a screw feeder using acoustic emissions, Powder Technology, Volume 336, August 2018, pp. 122-130
https://doi.org/10.1016/j.powtec.2018.05.029